Lasing threshold doubling at the crossover from strong to weak coupling regime in GaAs microcavity

New Journal of Physics
The open-access journal for physics

Lasing threshold doubling at the crossover from strong to weak coupling regime in GaAs microcavity

P Tsotsis[1,2], P S Eldridge[2,4], T Gao[1,2], S I Tsintzos[2], Z Hatzopoulos[2,3] and P G Savvidis[1,2]

[1] Department of Materials Science and Technology, University of Crete, 71003 Heraklion, Crete, Greece
[2] FORTH-IESL, PO Box 1385, 71110 Heraklion, Crete, Greece
[3] Department of Physics, University of Crete, 71003 Heraklion, Crete, Greece
E-mail: eldridge@physics.uoc.gr

New Journal of Physics **14** (2012) 023060 (12pp)
Received 23 October 2011
Published 29 February 2012
Online at http://www.njp.org/
doi:10.1088/1367-2630/14/2/023060

Abstract. In a polariton, laser coherent monochromatic light is produced by a low-energy state of the system at the bottom of a polariton 'trap', where a condensate of polaritons is formed, requiring no conventional population inversion. Following the recent realization of polariton light-emitting diodes (LEDs) based on GaAs microcavities (MCs) operating up to room temperature, efforts have been directed towards the demonstration of an electrically injected polariton laser. However, until now, low-threshold polariton lasing in GaAs MCs under optical pumping has been reported only at low temperatures. Here, we investigate the temperature dependence of lasing threshold across the border of the strong-to-weak coupling regime transition in high-finesse GaAs MCs under non-resonant optical pumping. Remarkably, we find that although lasing in the strong coupling regime is lost when the temperature is raised from 25 to 70 K, the threshold only doubles, in stark contrast with the expected difference of two orders of magnitude. Our results can be explained by considering temperature-induced thermalization of carriers to high wavevector states, increasing the reservoir's overall carrier lifetime, resulting in an order of magnitude higher steady-state carrier density at 70 K under similar pumping conditions.

[4] Author to whom any correspondence should be addressed.

Contents

1. Introduction

Exciton polaritons result from the strong coupling between a resonant optical cavity mode (CM) and a confined exciton. The bosonic nature of exciton polaritons inherited from their light–matter composition is responsible for observations of stimulated scattering [1, 2], amplification [3–5,], condensation [6–8] and lasing [9, 10] of polaritons. In contrast to conventional lasing, where coherent light emission is driven by stimulated photon emission, polariton lasing is achieved through the stimulated scattering of polaritons and the formation of a condensate (figure 1(a)) without the need for population inversion [11]. Therefore, polariton lasing promises two orders of magnitude lower threshold than conventional photon lasing [12] and a new generation of ultralow threshold laser devices. In addition, polariton condensates have been shown to exhibit similarities to atomic Bose–Einstein condensates (BECs), displaying a spontaneous build-up of long-range spatial coherence and a thermalized distribution within the population [6]. Unlike atomic BECs, polariton condensation can be achieved at high temperatures due to the very small polariton effective mass. The prospect of both ultralow threshold lasing and high-temperature macroscopic quantum phase makes the realization of an electrically driven polariton laser and condensate highly attractive.

The last few years have seen significant progress towards an electrically injected polariton laser based on GaAs microcavities (MCs). The observation of polariton lasing in a planar GaAs MC under non-resonant optical pumping, where carriers have comparable excess energy to those injected electrically, demonstrates the proof of concept [13]. There has also been progress in the electrical injection of polaritons, with reports of polariton LEDs [14–16], which can operate up to room temperature [17]. Following demonstrations of electroluminescence, experimental efforts have started to focus on polariton devices that permit electrical control of polaritons, including optical bistability [18] and polariton scattering [19]. This progress is encouraging as electrical control of hybrid Tamm plasmon exciton polaritons promises all optical circuits utilizing polariton neurons in MCs [20, 21].

Despite this progress, the realization of an electrically pumped polariton laser remains elusive. One obstacle is that the series resistance of the p-doped distributed Bragg reflector (DBR) inhibits efficient carrier injection at low temperatures (<50 K), where polariton lasing in a GaAs MC has been observed [13]. A second obstacle is that the energy bottleneck impedes the relaxation of hot polaritons to the centre of the polariton trap within the cavity photon lifetime (typically 1–2 ps). The latter can be addressed either by increasing the cavity photon lifetime, through the use of high-quality (Q) factor cavities, and/or by improving the efficiency of polariton relaxation in the linear regime, where phonon scattering dominates. Phonon-induced relaxation can be enhanced through polariton confinement [22], for example, by using micropillars [23] or by engineering MCs with additional relaxation channels based on

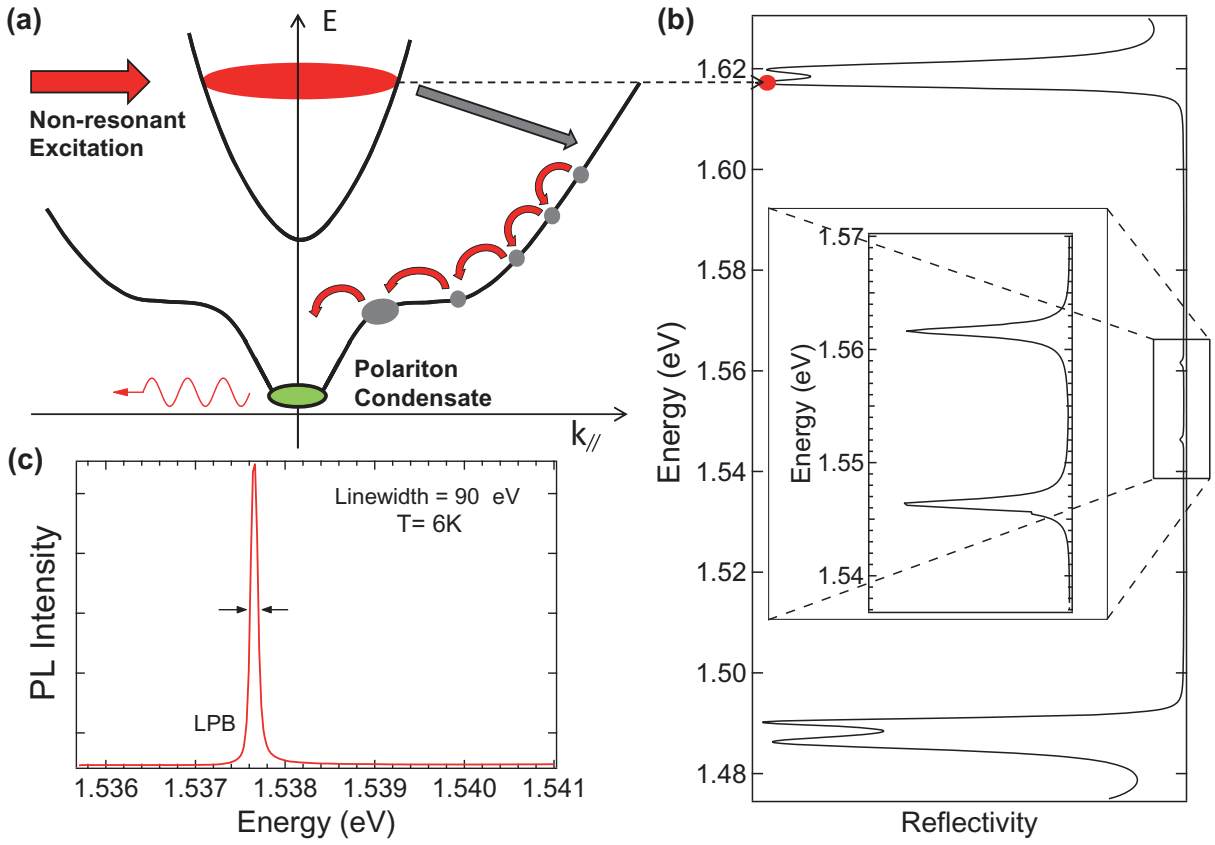

Figure 1. (a) The non-resonant pumping scheme used in this work and the relaxation processes that lead to polariton lasing. (b) The reflectivity and polariton modes for the high-Q microcavity calculated using the transfer matrix method. (c) Measured PL for a large negative detuning showing emission from the LPB.

longitudinal optical phonon resonance [24, 25]. However, before intensive efforts are put into designing electrically injected polariton lasers, an understanding is needed of what causes the onset of weak coupling lasing at higher temperatures in planar GaAs MCs and how optimized thresholds for strong and weak coupling lasing compare. A previous work on the temperature dependence of nonlinear gain in MCs in the strong coupling regime was conducted using resonant excitation [5], which, despite revealing interesting physics, does not provide conditions comparable to electrical injection. The non-resonant excitation experiments performed to date have been restricted to the strong coupling regime [13, 24, 26, 27] or examine the transition to the weak coupling regime and threshold dependence only at a given temperature [1, 23, 28, 29].

In this paper, we study the dependence of lasing threshold on temperature across the border of the strong to weak coupling regime transition in high-Q GaAs MCs under non-resonant optical pumping. Our results show that despite the loss of the strong coupling regime at high temperatures, the corresponding lasing threshold is only doubled, in stark contrast to previous reports comparing lasing thresholds in the two regimes at the same temperature [12, 30]. We present a simple model that takes into account changes in the reservoir lifetime due to thermalization of carriers to high wavevector states at high temperatures, which predicts an

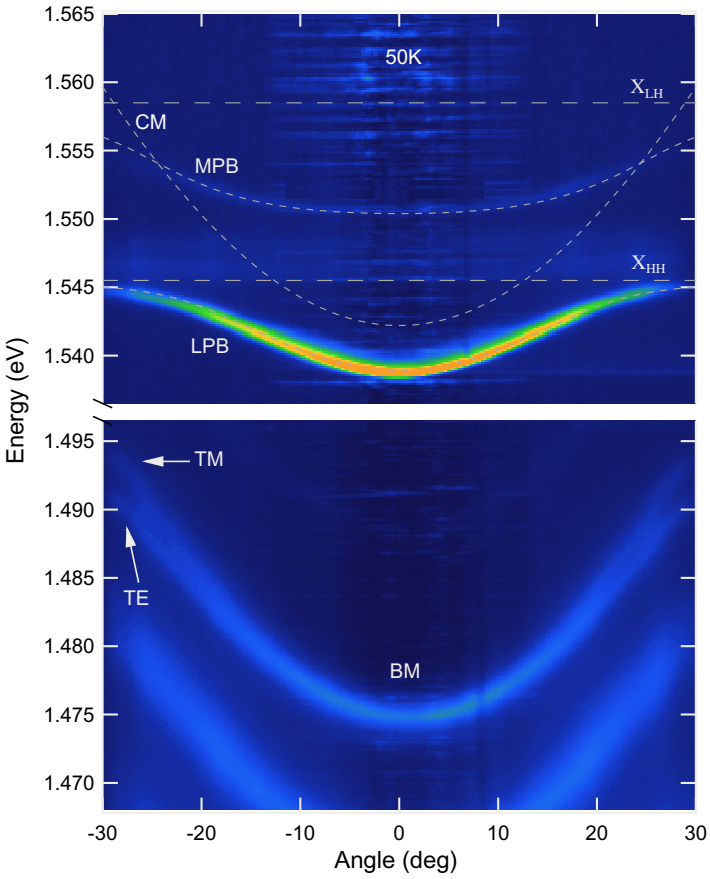

Figure 2. A far-field image (50 K) showing emission from the polariton branches (top) and the BM (bottom).

order of magnitude higher steady-state carrier density at 70 K under similar pumping conditions and explains this unexpected result.

2. Experiment

The sample is a high-Q 5/2 λ $Al_{0.3}Ga_{0.7}As$ MC with a top (bottom) DBR comprising 32 (35) repeats of $AlAs/Al_{0.15}Ga_{0.85}As$. Figure 1(b) shows the calculated reflectivity and polariton modes using the transfer matrix method. A wedge in the sample thickness allows the detuning (δ) between the CM and the heavy hole exciton (X_{HH}) to be varied, where $\delta = E_{CM} - E_{XHH}$ at zero in-plane wavevector ($k = 0$). To minimize the exciton density for a given polariton density, four sets of three 10 nm $Al_{0.3}Ga_{0.7}As/GaAs$ quantum wells (QWs) are placed at the antinodes of the cavity electric field.

The microcavity is mounted in a closed-cycle cryostat and excited non-resonantly, in a local minimum of the DBR reflectivity (see figure 1(b)) with the output from a Ti:sapphire in continuous wave (CW) operation. A microscope objective (numerical aperture = 0.546) is used to excite (spot size 40 μm) and collect light from the microcavity. The emission is focused onto the entry slit of a monochromator, which is coupled with a nitrogen-cooled silicon charge-coupled device (CCD). Far-field imaging is used to angularly resolve the emission, which enables direct measurement of the polariton dispersion (see figure 2) as the in-plane wavevector

is conserved in the emission process. At a low temperature (25 K) the formation of a real-space image in conjunction with a pinhole allows spatial filtering of the emission. The magnification and pinhole used correspond to collection of light from a 5 μm area on the sample, ensuring a constant laser power density within the collection area.

Figure 1(c) shows the photoluminescence (PL) emission at 6 K for a very negative detuning ($\delta = -9.7$ meV) where the lower polariton branch (LPB) has a large photonic fraction (0.88). The linewidth of 90 μeV corresponds to an experimental Q-factor of at least 16 000 in close agreement with the theoretical value of 20 000.

Figure 2 shows a typical image of the far-field emission at 50 K without spatial filtering and below threshold for $\delta = -3.3$ meV. The dashed lines are theoretical fits produced using the coupled oscillator model [25] that includes both heavy-hole (X_{HH}) and light-hole (X_{LH}) exciton states. Emission from the LPB and the middle polariton branch (MPB) in the top half of the image confirms the existence of the strong coupling regime. From the fits we calculate an effective Rabi splitting (Ω) at low excitation power of 9 meV. The bottom half of the image shows emission from the first low-energy Bragg mode (BM), which is split due to the polarization splitting in the cavity for the transverse electric (TE) and transverse magnetic (TM) optical modes.

To establish the nature of lasing in the sample, images are recorded above and below threshold for 25 and 70 K (figure 3). Figures 3(a) and (b) depict the emission below and above threshold for 25 K ($\delta = -4$ meV) with spatial filtering; the top half of both images (above the solid black line) are taken with longer exposure times. Below threshold the measured dispersion shows clear signatures of strong coupling; with emission from both MPB and LPB and the LPB relaxation bottleneck visible at high angles. Above threshold (figure 3(b)) the lasing emission comes from the LPB state blue shifted by ~ 1 meV. Emission from the MPB in the top part of the image provides definitive proof that the laser emission originates from exciton–polaritons in the strong coupling regime, as the spatial filtering prohibits the co-existence of both regimes within the collection area.

Figure 3(c) shows the far-field emission for 70 K ($\delta = -1$ meV) below threshold and displays similar features to those observed at 25 K, with emission from the LPB and MPB. Above threshold (figure 3(d)) we observe qualitatively different laser emission, with the emission originating from CM, a clear indicator that strong coupling has been lost. Additional images taken at a range of temperatures show strong coupling lasing up to 50 K, after which the lasing emission originates from the CM, in agreement with earlier studies in GaAs [13]. We note that no spatial filtering was performed at 70 K to allow easier comparison of the dispersions from the weakly coupled inner part of the excitation spot and the outer parts where the strong coupling regime remains intact.

We now turn our attention to the lasing performance of the two different regimes and compare power densities at the lasing threshold. The detuning of the sample is optimized to produce the lowest power density threshold for both 25 K ($\delta = -4.8$ meV) and 70 K ($\delta = -5.0$ meV), and PL is recorded from $k = 0$ in the absence of the pinhole to allow comparison of the lasing output power. These optimal detunings are consistent with earlier reports on strong coupling lasing [13] and reports of bandgap renormalization in VCSELs for conventional lasing in the low carrier density limit [31, 32]. Figures 4(a) and (b) show the integrated PL intensity and linewidth as a function of power for both 25 K (circles) and 70 K (squares). At 25 K there is a clear double threshold, the first corresponding to the onset of polariton lasing marked by a reduction in the LP linewidth (figure 4(b)) and the second to the onset of conventional

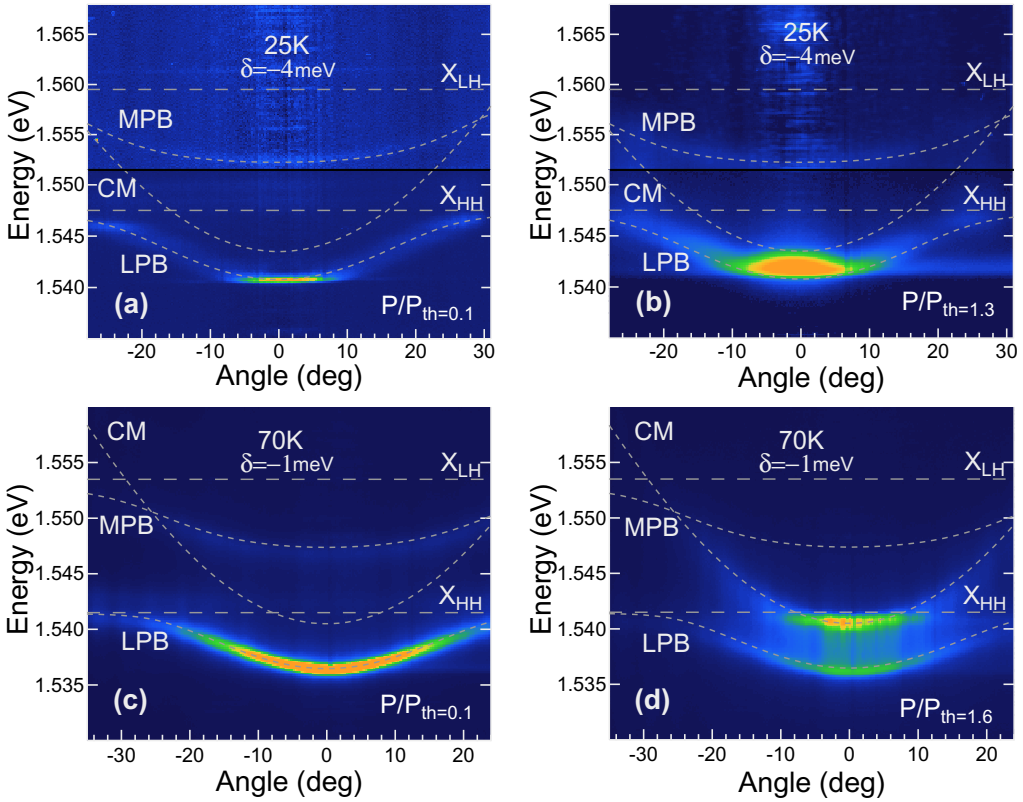

Figure 3. Far-field emission measured at 25 K (with spatial filtering) and 70 K (without) below (a, c) and above (b, d) threshold and theoretical fits (dashed lines). The top half of (a) and (b) have longer exposure times to clearly resolve the MPB. The apparent broadening of the polariton branches at high angles in (a) and (b) is a consequence of the reduction in the angular resolution from the spatial filtering. As spatial filtering was not used for 70 K, the emission from the LPB above threshold is from the outer regions of the excitation spot, where the carrier density is lower. We note that the image at the position of lasing in figure 3(b) is oversaturated in order to reveal emission from higher energy states along the LPB.

photon lasing, in agreement with past demonstrations of polariton lasing [23]. We note that the power density at threshold of about 640 W cm^{-2} is comparable to those reported under CW non-resonant excitation in both GaAs micrcopillars [23] and a planar high-Q microcavity [13].

At 70 K we observe a single threshold as expected for weak coupling lasing. Remarkably, the power density at the onset of weak coupling lasing of 1300 W cm^{-2} is only double the power density in the strong coupling regime at 25 K. This is in stark contrast to the commonly expected two orders of magnitude difference in threshold power between polariton laser and conventional photon lasing as observed in [12] at low temperatures. As we show below, threshold power that is important for device applications is not necessarily proportional to threshold carrier density which defines the physical regime of the lasing process. This difference only becomes apparent when the temperature is varied, as an increase in the mean carrier lifetime breaks the one-to-one correspondence between the threshold power and the threshold carrier density. Thus despite

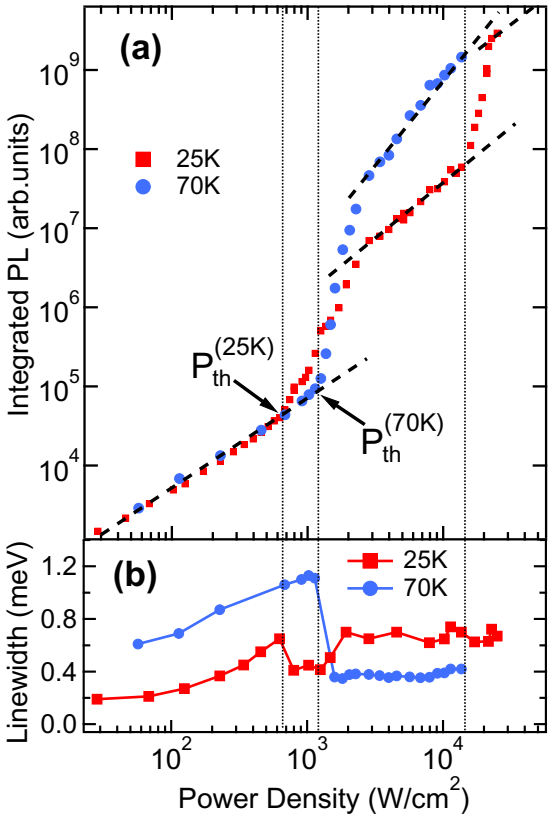

Figure 4. (a) The integrated PL with increasing power density, showing a clear lasing transition for 25 K (red squares) and 70 K (blue circles) temperatures. The power dependence shows a nearly linear power dependence, which is characteristic of the predominantly acoustic phonon relaxation mechanism. (b) The corresponding linewidths with increasing power density.

having similar pumping thresholds the carrier density at high temperatures can be significantly different from that at low temperatures, leading to the collapse of the strong coupling regime.

3. Discussion and conclusion

Here, we examine different contributing factors to the reduction of Rabi splitting and confirm that a temperature-dependent carrier lifetime can account for the observed loss of strong coupling lasing at 70 K. We first consider the effect of temperature and doubling of the carrier density on the effective Rabi splitting in our high-Q microcavity, assuming the same radiative carrier lifetimes at 25 and 70 K (0.7 ns). The temperature dependence of the Rabi splitting ($\Omega(T)$) can be approximated using the equation $\Omega(T) = \sqrt{4V^2 - (\gamma_{ex}(T) - \gamma_c)^2}$, where V represents the coupling strength between the CM and the exciton, and $\gamma_{ex} = 1.1$ meV, $\gamma_C = 0.09$ meV are the exciton and cavity linewidths, respectively [33]. A reduction in $\Omega(T)$ and therefore the onset of weak coupling can result from a decrease in V through a reduction of the exciton oscillator strength with increasing carrier density. Assuming 2% absorption per

QW [34], we estimate a carrier density of $2 \times 10^{10}\,\mathrm{cm}^{-2}$ per QW for the lasing threshold at 25 K, below the saturation density of $n_{\mathrm{sat}} \sim 5 \times 10^{10}\,\mathrm{cm}^{-2}$ for this system [35]. A straightforward calculation shows that doubling of the carrier density would not reduce the exciton oscillator strength sufficiently to cause loss of strong coupling and the onset of conventional photon lasing.

Another mechanism for the reduction of $\Omega(T)$ is by increasing the exciton linewidth (γ_{ex}) through both phonon and collision broadening. Phonon broadening of the heavy-hole transition in QWs has been shown to only become significant above 100 K [17, 36], and is negligible between 25 and 70 K, rendering it incapable of inducing weak coupling. Similarly, previous reports have suggested that collision broadening for these negative detunings has a small effect on the lower polariton linewidth due to the reduced density of states in the strong coupling region [37] and short polariton lifetimes not allowing efficient relaxation of polaritons into the trap. In contrast, in our high-Q MC sample the increased polariton lifetimes allow sufficient time for polaritons to scatter on the LPB, leading to the onset of polariton lasing. Such an enhanced relaxation inside the trap via acoustic phonons and polariton–polariton scattering necessary for polariton lasing is confirmed by polariton linewidth broadening just below threshold, as seen in figure 4(b). As we observe polariton lasing at 25 K, this broadening is insufficient to destroy the strong coupling regime. Although we expect an additional reduction in Rabi splitting at 70 K, the estimated twofold increase in carrier density at threshold cannot explain the observed transition to transparency and the onset of conventional lasing.

We next consider the effect of temperature on the average radiative lifetime of carriers in the system that defines the steady-state carrier density under continuous pumping conditions. Such temperature-dependent radiative lifetimes are well known for GaAs/AlGaAs QWs [38, 39] and have theoretically been calculated for exciton–polaritons [40]. Under non-resonant excitation, free electrons and holes are generated that cool rapidly to form excitons and then relax towards the polariton trap, becoming more photon-like in the process. When the temperature is increased, polaritons scatter to higher wavevectors into states with higher exciton fraction and reservoir states outside the light cone, where they are no longer coupled to light. The long lifetime of these high wavevector states ensures their thermalized population, whereas this is not necessarily the case for the small wavevector states where the relatively short radiative lifetimes hinder their efficient thermalization. We note that the average carrier lifetime is controlled by the distribution of carriers between different states and the lifetime of each state. Thus an increase in temperature leads to thermal redistribution of carriers towards high wavevector states, increasing the overall carrier lifetime, provided that non-radiative rates of these states remain unchanged for the temperature range considered. Although polariton relaxation inside the trap is also enhanced with increasing temperature, the polariton population around $k = 0$ constitutes only a small fraction of the overall carrier population, having little effect on the average carrier lifetime. Thus, for the same pumping rate, the steady-state carrier density is increased due to an increase in the effective carrier lifetime when the temperature is raised. This increase in density reduces the Rabi splitting through both a decrease of the exciton oscillator strength and further collision broadening of the exciton transition.

Figure 5 illustrates an estimation of the carrier density per QW for different powers and temperatures, assuming a linear increase of the lifetime (grey dashed line) theoretically calculated for polaritons in the linear regime [40][5]. The grey squares represent measured

[5] Although this calculation ignores exciton ionization that occurs at higher temperatures, ionization would lead to a reservoir with an admixture of excitons and free electrons and holes. These free carriers are still long-lived, giving rise to a higher steady-state carrier density for similar pumping rates.

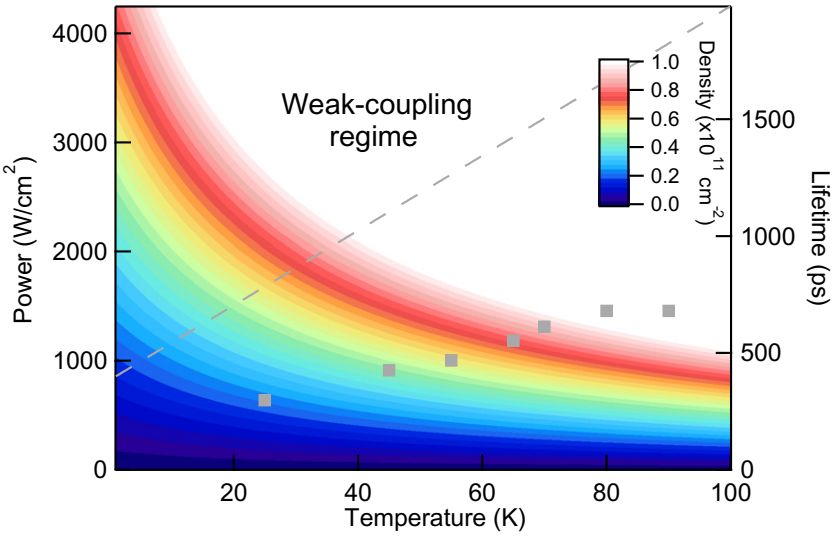

Figure 5. The estimated change in carrier density per QW with power and temperature considering a linear increase in the lifetime with temperature (dashed line). The squares represent the optimized lasing threshold measured at different temperatures.

optimized thresholds for a range of temperatures. We observe a clear increase in the strong-coupling lasing threshold with temperature (<50 K), consistent with past observations in GaAs, CdTe and GaN MCs at densities that scale according to their exciton binding energy [13, 26, 27]. We believe that, for these relatively small negative detunings, the increase in threshold can be attributed to the thermal excitation of polaritons out of the polariton trap [27] and the increase of critical density for condensation with temperature [41]. It is clear from figure 5 that even though the optical threshold powers are similar at 25 and 70 K, the carrier densities per QW are very different. We estimate that at 70 K the number of carriers per QW is double the saturation density, consistent with observations of the onset of weak coupling at densities just above the saturation density [28, 35].

We note that although this calculated increase in the steady-state density can explain the loss of strong coupling, the estimated threshold carrier density at 70 K is below the theoretical transparency density for 10 nm GaAs/AlGaAs QWs at 70 K (3×10^{11} cm^{-2} [42]). One possible explanation is an underestimation of the temperature dependence as the theoretical lifetime used in figure 5 is for a cavity with a Q-factor of a few thousand. As evidenced by the observation of polariton lasing, the long cavity photon lifetime enhances scattering within the polariton lifetime and the thermal spread of carriers. Another possibility is the presence of excitons in the QWs just after the loss of strong coupling. This may explain the low threshold carrier density, as a recent work has suggested that excitons can play a role in lasing in the weak coupling regime [43, 44]. Further experimental work is needed to investigate this intermediate regime, where lasing in the weak coupling regime appears to occur below transparency.

In conclusion, we present clear evidence for polariton lasing in a high-Q planar microcavity at low temperatures under non-resonant excitation. At higher temperatures we observe lasing in the weak coupling regime, which occurs at comparable thresholds. The loss of strong coupling with temperature we associate with the increase of the average carrier lifetime and

therefore density with temperature. The comparable thresholds for lasing at 25 and 70 K reveal an intriguing intermediate regime for low threshold lasing at increased temperatures. It is therefore clear that any realization of polariton-based devices requires a detailed comparison and understanding of different lasing regimes and of specific advantages these offer. We believe that further optimization of polariton injection towards more resonant schemes that utilize for example LO phonons [24, 25, 45] could lead to improved performance of polariton-based devices fulfilling their potential as novel ultralow threshold sources of monochromatic coherent light.

Acknowledgments

The authors acknowledge funding from the FP7 Clermont 4 and INDEX ITN projects and the POLATOM ESF Research Network Programme. This work was also co-funded by the EU and National Resources through the scientific program 'EPEAEK II-HRAKLEITOS II, University of Crete'. The authors thank Alexis Askitopoulos and Pavlos Lagoudakis for their assistance with the measurement of the sample Q-factor.

References

[1] Dang L S, Heger D, André R, Bœuf F and Romestain R 1998 Stimulation of polariton photoluminescence in semiconductor microcavity *Phys. Rev. Lett.* **81** 3920–3
[2] Senellart P, Bloch J, Sermage B and Marzin J 2000 Microcavity polariton depopulation as evidence for stimulated scattering *Phys. Rev.* B **62** R16263–6
[3] Savvidis P G, Baumberg J J, Stevenson R M, Skolnick M S, Whittaker D M and Roberts J S 2000 Angle-resonant stimulated polariton amplifier *Phys. Rev. Lett.* **84** 1547–50
[4] Ciuti C, Schwendimann P, Deveaud B and Quattropani A 2000 Theory of the angle-resonant polariton amplifier *Phys. Rev.* B **62** R4825–8
[5] Saba M *et al* 2001 High-temperature ultrafast polariton parametric amplification in semiconductor microcavities *Nature* **414** 731–5
[6] Kasprzak J *et al* 2006 Bose-Einstein condensation of exciton polaritons *Nature* **443** 409–14
[7] Deng H, Press D, Götzinger S, Solomon G, Hey R, Ploog K and Yamamoto Y 2006 Quantum degenerate exciton-polaritons in thermal equilibrium *Phys. Rev. Lett.* **97** 146402
[8] Baumberg J J *et al* 2008 Spontaneous polarization buildup in a room-temperature polariton laser *Phys. Rev. Lett.* **101** 136409
[9] Malpuech G, Di Carlo A, Kavokin A, Baumberg J J, Zamfirescu M and Lugli P 2002 Room-temperature polariton lasers based on GaN microcavities *Appl. Phys. Lett.* **81** 412
[10] Christopoulos S *et al* 2007 Room-temperature polariton lasing in semiconductor microcavities *Phys. Rev. Lett.* **98** 126405
[11] Imamoglu A, Ram R J, Pau S and Yamamoto Y 1996 Nonequilibrium condensates and lasers without inversion: exciton-polariton lasers *Phys. Rev.* A **53** 4250–3
[12] Deng H, Weihs G, Snoke D, Bloch J and Yamamoto Y 2003 Polariton lasing vs. photon lasing in a semiconductor microcavity *Proc. Natl Acad. Sci. USA* **100** 15318–23
[13] Wertz E, Ferrier L, Solnyshkov D D, Senellart P, Bajoni D, Miard A, Lemaître A, Malpuech G and Bloch J 2009 Spontaneous formation of a polariton condensate in a planar GaAs microcavity *Appl. Phys. Lett.* **95** 051108
[14] Tsintzos S I, Pelekanos N T, Konstantinidis G, Hatzopoulos Z and Savvidis P G 2008 A GaAs polariton light-emitting diode operating near room temperature *Nature* **453** 372–5

[15] Khalifa A A, Love A P D, Krizhanovskii D N, Skolnick M S and Roberts J S 2008 Electroluminescence emission from polariton states in GaAs-based semiconductor microcavities *Appl. Phys. Lett.* **92** 061107
[16] Bajoni D, Semenova E, Lemaître A, Bouchoule S, Wertz E, Senellart P and Bloch J 2008 Polariton light-emitting diode in a GaAs-based microcavity *Phys. Rev.* B **77** 113303
[17] Tsintzos S I, Savvidis P G, Deligeorgis G, Hatzopoulos Z and Pelekanos N T 2009 Room temperature GaAs exciton–polariton light emitting diode *Appl. Phys. Lett.* **94** 071109
[18] Bajoni D, Semenova E, Lemaître A, Bouchoule S, Wertz E, Senellart P, Barbay S, Kuszelewicz R and Bloch J 2008 Optical bistability in a GaAs-based polariton diode *Phys. Rev. Lett.* **101** 266402
[19] Christmann G, Coulson C, Baumberg J J, Pelekanos N T, Hatzopoulos Z, Tsintzos S I and Savvidis P G 2010 Control of polariton scattering in resonant-tunneling double-quantum-well semiconductor microcavities *Phys. Rev.* B **82** 113308
[20] Liew T C H, Kavokin A V, Ostatnický T, Kaliteevski M, Shelykh I A and Abram R A 2010 Exciton-polariton integrated circuits *Phys. Rev.* B **82** 033302
[21] Liew T C H, Kavokin A V and Shelykh I A 2008 Optical circuits based on polariton neurons in semiconductor microcavities *Phys. Rev. Lett.* **101** 016402
[22] Paraïso T K *et al* 2009 Enhancement of microcavity polariton relaxation under confinement *Phys. Rev.* B **79** 045319
[23] Bajoni D, Senellart P, Wertz E, Sagnes I, Miard A, Lemaître A and Bloch J 2008 Polariton laser using single micropillar GaAs–GaAlAs semiconductor cavities *Phys. Rev. Lett.* **100** 047401
[24] Boeuf F, Romestain R, André R, Si Dang L, Péronne E, Lampin J F, Hulin D and Alexandrou A 2000 Evidence of polariton stimulation in semiconductor microcavities *Phys. Rev.* B **62** R2279–82
[25] Maragkou M, Grundy A J D, Ostatnický T and Lagoudakis P G 2010 Longitudinal optical phonon assisted polariton laser *Appl. Phys. Lett.* **97** 111110
[26] Kasprzak J, Solnyshkov D D, André R, Dang L S and Malpuech G 2008 Formation of an exciton polariton condensate: thermodynamic versus kinetic regimes *Phys. Rev. Lett.* **101** 146404
[27] Levrat J, Butté R, Feltin E, Carlin J-F, Grandjean N, Solnyshkov D and Malpuech G 2010 Condensation phase diagram of cavity polaritons in GaN-based microcavities: experiment and theory *Phys. Rev.* B **81** 125305
[28] Houdré R, Gibernon J L, Pellandini P, Stanley R P, Oesterle U, Weisbuch C, O'Gorman J, Roycroft B and Ilegems M 1995 Saturation of the strong-coupling regime in a semiconductor microcavity: free-carrier bleaching of cavity polaritons *Phys. Rev.* B **52** 7810–3
[29] Butté R, Delalleau G, Tartakovskii a I, Skolnick M S, Astratov V N, Baumberg J J, Malpuech G, Di Carlo A, Kavokin A V and Roberts J S 2002 Transition from strong to weak coupling and the onset of lasing in semiconductor microcavities *Phys. Rev.* B **65** 205310
[30] Azzini S, Gerace D, Galli M, Sagnes I, Braive R, Lemaître A, Bloch J and Bajoni D 2011 Ultra-low threshold polariton lasing in photonic crystal cavities *Appl. Phys. Lett.* **99** 111106
[31] Gourley P L, Lyo S K, Brennan T M, Hammons B E, Schaus C F and Sun S 1989 Lasing threshold in quantum well surface-emitting lasers: many-body effects and temperature dependence *Appl. Phys. Lett.* **55** 2698–700
[32] Tomita A and Suzuki A 1987 Carrier-induced lasing wavelength shift for quantum well laser diodes *Quantum Electron. IEEE J. Quantum Electron.* **23** 1155–9
[33] Kavokin A V, Baumberg J J, Malpuech G and Laussy F P 2007 *Microcavities* (New York: Oxford University Press)
[34] Masselink W T, Pearah P J, Klem J, Peng C K, Morkoç H, Sanders G D and Chang Y Y-C 1985 Absorption coefficients and exciton oscillator strengths in AlGaAs-GaAs superlattices *Phys. Rev.* B **32** 8027–34
[35] Rhee J-K, Citrin D S, Norris T B, Arakawa Y and Nishioka M 1996 Femtosecond dynamics of semiconductor-microcavity polaritons in the nonlinear regime *Solid State Commun.* **97** 941–6
[36] Gammon D, Rudin S, Reinecke T L and Katzer D S 1995 Phonon broadening of excitons in GaAs/Al_xGa_{1-x} As quantum wells *Phys. Rev.* B **51** 16785
[37] Ciuti C, Savona V, Piermarocchi C, Quattropani A and Schwendimann P 1998 Threshold behavior in the collision broadening of microcavity polaritons *Phys. Rev.* B **58** R10123–6

[38] Feldmann J, Peter G, Göbel E O, Dawson P, Moore K, Foxon C and Elliott R J 1987 Linewidth dependence of radiative exciton lifetimes in quantum wells *Phys. Rev. Lett.* **59** 2337–40

[39] Gurioli M, Vinattieri A, Colocci M, Deparis C, Massies J, Neu G, Bosacchi A and Franchi S 1991 Temperature dependence of the radiative and nonradiative recombination time in GaAs/$Al_xGa_{1-x}As$ quantum-well structures *Phys. Rev.* B **44** 3115–24

[40] Savona V, Piermarocchi C, Quattropani A, Schwendimann P, Tassone F and Taylor P 1999 Optical properties of microcavity polaritons *Phase Transit.* **68** 169–279

[41] Malpuech G, Rubo Y G, Laussy F P, Bigenwald P and Kavokin A V 2003 Polariton laser: thermodynamics and quantum kinetic theory *Semicond. Sci. Technol.* **18** S395–404

[42] Chow W W and Koch S W 1999 *Semiconductor Laser Fundamentals* (Berlin: Springer)

[43] Guillet T, Brimont C, Valvin P, Gil B, Bretagnon T, Médard F, Mihailovic M, Zúñiga-Pérez J, Leroux M, Semond F and Bouchoule S 2011 Laser emission with excitonic gain in a ZnO planar microcavity *Appl. Phys. Lett.* **98** 211105

[44] Kammann E, Maragkou M, Grundy A J D, Kavokin A V and Lagoudakis P G 2011 Crossover from exciton-polariton to photon Bose–Einstein condensation arXiv:1103.4831

[45] Somaschi N, Mouchliadis L, Coles D, Perakis I E, Lidzey D G, Lagoudakis P G and Savvidis P G 2011 Ultrafast polariton population build-up mediated by molecular phonons in organic microcavities *Appl. Phys. Lett.* **99** 143303